Performance Evaluation of Synchronization Method for Reducing the Overall Synchronization Time in Digital Radio Mondiale Receivers

Ki-Won Kwon[1], Seong-Jun Kim[1], Jun Hwang[2], and Jong-Ho Paik[2]
[1]Mobile Convergence Platform Research Center, Korea Electronics Technology Institute
Seoul 121-835, Republic of Korea
[e-mail: {kwonkw, ksjuny}@keti.re.kr]
[2] Department of Multimedia, Seoul Women's University
Seoul 139-774, Republic of Korea
[e-mail: {hjun, paikjh}@swu.ac.kr]
*Corresponding author: Jong-Ho Paik

Received April 24, 2013; revised July 8, 2013; accepted July 31, 2013; published August 30, 2013

Abstract

In this paper, we present a comparative performance evaluation of the sampling frequency synchronization method that eliminates the initial sampling frequency offset (SFO) to reduce the overall synchronization time in Digital Radio Mondiale (DRM) receivers. To satisfy the advanced synchronization performance requirements of DRM receivers, we introduce the conventional DRM synchronization method (Method 1) and another method (Method 2), which does not perform the initial sampling frequency synchronization in the conventional synchronization method (both methods are mentioned later in this paper). To demonstrate the effectiveness of the performance evaluation, analytical expressions for frame detection are derived and simulations are provided. Based on the simulations and numerical analysis, our result shows that Method 2, with a negligible performance loss, is robust to the effects of the initial sampling frequency synchronization even if SFO is present in the DRM signal. In addition, we verify that the inter-cell differential correlation used between reference cells is robust to the effect of the initial SFO.

Keywords: DRM, Frame Detection, Synchronization

This work was supported by a special research grant from Seoul Women's University (2013).

http://dx.doi.org/10.3837/tiis.2013.08.007

1. Introduction

Orthogonal frequency division multiplexing (OFDM) has been chosen as the transmission method for several broadcasting standards such as digital radio broadcasting (DAB), digital video broadcasting, and DRM. DRM is an OFDM-based international DAB standard that can substitute for analog AM radio in frequency bands below 120 MHz [1]. DRM has caught the attention of broadcasters throughout the world because of its broad coverage. At present, DRM is being used in various regions around the globe, such as in Europe and Asia. According to DRM Consortium, DRM broadcast infrastructure is being established in India and Russia as a result of their recent decision to adopt DRM-based digital radio.

The adoption of DRM is expected to grow and expand globally in the future. To use DRM broadcast services, a DRM receiver must receive the broadcast signal, convert it into a baseband digital signal, and perform preprocessing operations on the signal, which include synchronization, equalization, decoding, and parsing. Therefore, an unavoidable delay is involved from the moment the user powers up the device to play a sound or invoke a data service. In an AM or FM analog radio, audio services start immediately after tuning into a particular frequency. Because this delay does not occur in analog broadcast receivers, it has become a key performance evaluation element of the receiver, and DRM receiver engineers must consider the receiver time delay as a receiver design parameter. DRM uses OFDM modulation, which is sensitive to the frequency synchronization error caused by the difference between the oscillators at the transmitter and receiver [2,3]. Therefore, frequency offset synchronization is one of the most important procedures for OFDM-based DRM systems. The carrier frequency offset (CFO) is usually divided into a fractional and an integer part. The integer frequency offset (IFO) results in a shift in the subcarrier indexes, and the fractional frequency offset causes inter-carrier interference because of the loss in orthogonality at the receiver. Several schemes have been proposed in the literature for synchronization [4].

The DRM receiver synchronization consists of several synchronization steps relative to the symbol time, carrier frequency, and sampling frequency. Therefore, it is possible to improve algorithmically the processing speed as compared with the other pre-processing operations such as decoding and data parsing [5].

For the DRM synchronization, each of symbol time synchronization, fractional frequency synchronization and sampling frequency synchronization was operated in serial order in the time domain, and initial synchronization method for the integer frequency synchronization and frame detection was suggested in the frequency domain [6]. However, this method was not suitable for high speed synchronization because multiple OFDM symbols have to be used in the SFO estimation process for the initial frequency synchronization. Another synchronization method which is the simultaneous separation and estimation of more than two synchronization parameters from the same signal was suggested. In this method, symbol duration with CFO or carrier frequency with SFO synchronization was simultaneously estimated [7, 8]. And the implementation of this method in the parallel processing structure possibly reduces of necessary estimated steps for the initial synchronization. However, this algorithm was not considered in this study. The reason is that unlike estimation algorithm that is based on the regular training symbol or pilot-based Burst Mode OFDM communication for the frequency synchronization, this method is not suitable for random pilot-based continuous mode like DRM broadcasting systems.

The DRM standard uses reference cells that perform the same function as the OFDM pilots for synchronization. Initial synchronization is carried out by selecting a method that conforms to the DRM specification from existing initial synchronization methods based on OFDM pilot symbols or by changing an existing method to meet the DRM specification requirements.

In this paper, we present a comparative performance evaluation of the sampling frequency synchronization method, which eliminates the initial SFO to reduce the overall synchronization time in the DRM receivers. To demonstrate the effectiveness of the performance evaluation, analytical expressions for frame detection are derived and simulations are provided.

The rest of this paper is organized as follows. In Section 2, a system model for the DRM and a signal model for OFDM-based DRM systems are presented. In Section 3, the conventional DRM synchronization method and another method that eliminates the initial SFO process in the conventional synchronization method are introduced; their performance is numerically analyzed. In Section 4, the performance evaluation through simulation results are presented. Finally, Section 5 concludes this paper.

2. System and Signal Models

2.1 System Model

DRM is highly frequency efficient because it uses OFDM modulation. It can easily deal with frequency-selective fading. However, on the downside, its overall reception performance fluctuates depending on the synchronization performance. The DRM physical layer is designed to provide a spectrum efficiency greater than 2 bits/(s·Hz) in the 9- to 10-kHz AM band for high-quality audio services in the diverse transmission environment of the AM frequency band. The transmission frame structure consists of the fast access channel (FAC), which contains the channel information and service-relevant information required by the receiver; the main service channel (MSC), which carries the audio and data payload; and the service description channel (SDC), which carries the channel-coding parameters for the MSC and the multiplex structure of the audio and data signals. Transmission modes A–D have a super frame of 1,200 ms, which consists of three 400-ms frames. Transmission mode E, also known as DRM+, has a super frame size of 400 ms, which consists of four 100-ms frames. **Fig. 1** shows the structure of the super frame, which consists of 15–24 OFDM symbols per frame, depending on the transmission mode. The first two to three OFDM symbols of each super frame carry the SDC. The remaining OFDM symbols carry the MSC and FAC. To receive in the DRM, frame synchronization must be performed to detect the start of a frame.

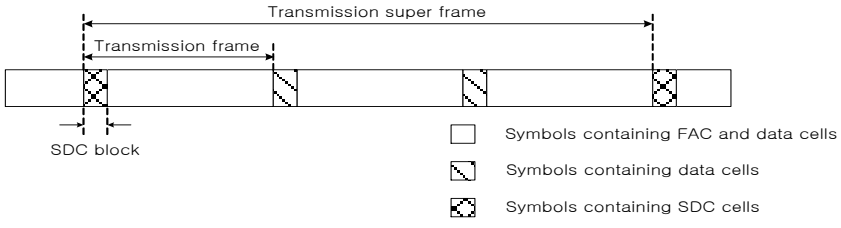

Fig. 1. Transmission frame structure.

Five transmission modes determined by the frequency characteristics of the DRM services are defined to effectively handle the diverse terrestrial transmission environment. **Table 1**

shows the OFDM parameters for each mode. Transmission modes A–D support digital radio in the AM bands below 30 MHz. Transmission mode E provides digital radio in the 30- to 174-MHz frequency bands. For bands below 30 MHz, transmission mode A is the most favorable radio environment, and transmission mode D is the worst. For bands between 30 and 174 MHz, only mode E can be selected. Mode E is designed to be robust to time and the frequency-selective fading channel [1]. Depending on the mode used, the spectrum occupancy can be set to 4.5/5/9/10/18/20/100 kHz. The spectrum occupancy information is transmitted in the FAC. Therefore, if the FAC is decoded without any error in the 4.5-kHz bandwidth from the center frequency during the synchronization, channel estimation of the designated occupied bandwidth can be carried out after obtaining the occupied-bandwidth information from the FAC. DRM defines the reference cells to perform synchronization and channel estimation. The frequency reference cell is always located in the subcarrier frequencies corresponding to 750, 2,250, and 3,000 Hz of each OFDM symbol, and it is used for frequency synchronization. **Fig. 2** shows the three types of reference cells. The time reference cell exists only in the first OFDM symbol of each transmission frame, and it is used for frequency and frame synchronization. The gain reference cell is split in each OFDM symbol, and it is used for channel estimation. All reference cells have a coefficient of $\sqrt{2}$, and the gain reference cells located at the extremes have a coefficient of two [1,9].

Table 1. DRM OFDM parameters

Parameter	A	B	C	D	E
T (μs)	$83^{1/3}$	$83^{1/3}$	$83^{1/3}$	$83^{1/3}$	$83^{1/3}$
Useful Symbol Duration, T_u (ms)	24	$21^{1/3}$	$14^{2/3}$	$9^{1/3}$	$2^{1/4}$
Guard Interval T_g (ms)	$2^{2/3}$	$5^{1/3}$	$5^{1/3}$	$7^{1/3}$	$0^{1/4}$
T_g/ T_u	1/9	1/4	4/11	11/14	1/9
OFDM Symbol Duration (ms)	$26^{2/3}$	$26^{2/3}$	20	$16^{2/3}$	$2^{1/2}$
Frame Duration (ms)	400				100

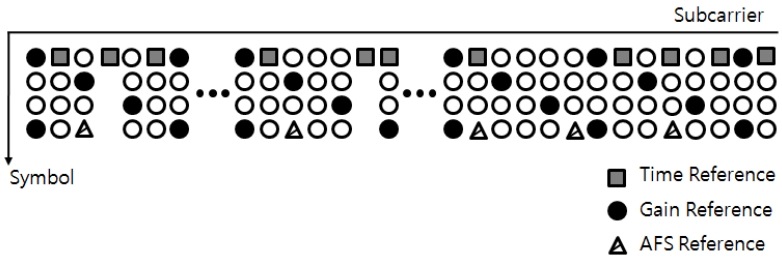

Fig. 2. Reference cell structure.

2.2 Signal Model

If the initial SFO estimation and correction processes are omitted and integer CFO estimation and frame detection are carried out after a fast Fourier transform (FFT) for initial high-speed synchronization in the DRM receivers, the DRM performance is influenced by the initial SFO, and the degree of this influence depends on the characteristics of the algorithm used. Therefore, it is important to select an algorithm that is robust to the effects of the initial SFO to achieve more accurate IFO estimation and frame detection. In this study, we compare and analyze two reference-cell-based correlation methods suitable for application to OFDM symbols in the frequency domain after FFT. Because the effects of SFO equally influence both the IFO and frame-detection processes, only the frame detection process is observed. The simplest reference-cell-based correlation method is to use the correlation between the reference cell and the received signal. Assuming ideal symbol timing synchronization, the *l*th OFDM reception symbol after FFT influenced by the SFO can be represented as follows [10,11]:

$$R_l(k) = \alpha(\xi \cdot N_s \cdot l) \cdot e^{j\pi\phi_k} \cdot e^{j2\pi(\xi \cdot N_s \cdot l)k/N} \cdot e^{j2\pi\left(\left(lN_s + N_g\right)/N\right)\phi_k} \cdot X_l(k) \cdot H_l(k) + N_l(k) \quad (1)$$

where ξ is the SFO and $\alpha(.)$ is the distortion coefficient of the subcarrier due to the SFO. $e^{j2\pi(\xi \cdot N_s \cdot l)k/N}$ represents the phase coefficient due to the SFO. $X_l(k)$ is the data symbol assigned to the *k*th subcarrier in the *l*th OFDM symbol transmitted. N, N_g, and N_s represent the FFT size. $N_s = N_g + N$. ϕ_k is generally expressed as the residual CFO and sampling time offset (STO); because STO is zero, it can be approximated as the residual frequency offset ϵ. $H_l(k)$ and $N_l(k)$ represent the channel frequency response and noise, respectively.

3. Performance Evaluation of SFO Synchronization Methods in DRM Receivers

3.1 Method 1: Nogami Method

The conventional synchronization method of DRM is summarized in this section. First, we detect the five DRM transmission modes. Transmission-mode detection is achieved by obtaining the correlation of the received signal using the guard interval and useful symbol duration for each mode. Once the transmission mode has been determined, synchronization is carried out using the reference cells located within 4.5 kHz from the center frequency regardless of the multiple-occupancy bandwidths. Coarse symbol timing synchronization is performed, which is later corrected by fractional CFO estimation. Then, after the SFO estimation and correction, the signal is changed into the frequency domain through FFT, and IFO estimation and frame detection are performed. The timing and frequency offsets are continuously tracked after the initial synchronization process described earlier [6]. Initial sampling frequency synchronization is performed to estimate and correct the initial SFO caused by the use of low-cost oscillators in many conventional DRM receivers. However, the initial synchronization process takes longer because the SFO estimation and correction are necessary for the sampling frequency synchronization. This process in turn means delayed service start time for the users. **Fig. 3** shows the general synchronization process of the DRM received signal.

For evaluation, we define Method 1 using the correlation value between the reference cell and the received symbol and express it as follows [12]:

$$\hat{l}_1 = \arg\max_{l_1} \left| \sum_{k=1}^{N_{RC}} R_{l_1}\left(P_{RC}[k]\right) \cdot X_{l_1}{}^{*}\left(P_{RC}[k]\right) \right| \tag{2}$$

where $l_1 = 0, 1, 2, \ldots, S_n\text{-}1$ and S_n is the number of OFDM symbols per frame. $P_{RC}[k]$ is the position of the kth reference cell. $R_l(P_{RC}[k])$ is the kth reference cell of the lth symbol received. $X(P_{RC}[k])$ is the kth reference cell transmitted, i.e., a known reference cell. N_{RC} refers to the number of all reference cells within the 0- to 4.5-kHz bandwidth. To analyze Equation (2), Equation (1) is substituted into Equation (2) as follows:

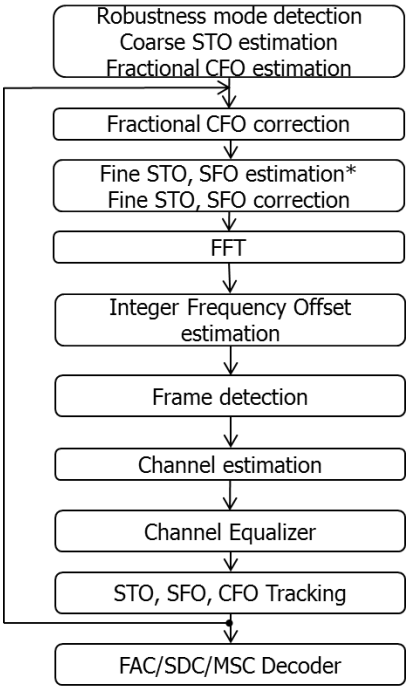

Fig. 3. General synchronization process of the DRM received signal.

$$\begin{aligned}\hat{l}_1 &= \arg\max_{l_1} \frac{N-\xi\cdot N_s\cdot l}{N}\cdot e^{j2\pi(l\cdot N_s/N)\varepsilon}\left|\sum_{k=1}^{N_{RC}} e^{j2\pi(\xi\cdot N_s\cdot l_1)P_{TRC}[k]/N}\cdot H_{l_1}(P_{RC}[k])\right| \\ &= \arg\max_{l_1} \beta_{l_1}\cdot\left|\Gamma_{l_1}\right|\end{aligned} \tag{3}$$

where $\beta_{l_1} = \frac{N-\xi\cdot N_s\cdot l}{N}\cdot e^{j2\pi(l\cdot N_s/N)\varepsilon}$ and $\Gamma_{l_1} = \sum_{k=1}^{N_{RC}} e^{j2\pi(\xi\cdot N_s\cdot l_1)P_{TRC}[k]/N}\cdot H_{l_1}(P_{RC}[k])$. The residual frequency offset value (ϵ) and the SFO in β_{l_1} are very small [in parts per million (ppm)]. Therefore, the approximations $\xi \lll 1$ and $\beta_{l_1} \approx 1$ hold. Applying these approximations to Equation (3) yields the following equation:

$$\hat{l}_1 = \arg\max_{l_1} \left|\Gamma_{l_1}\right| . \tag{4}$$

The reference cell is aperiodic and located irregularly. Therefore, $P_{RC}[k]$ in Γ_{l_1} can be spread in all FFT areas and is influenced greatly by the SFO. **Fig. 4** shows the distribution of the phase shift assuming an ideal channel, and **Fig. 5** shows the same distribution assuming perfect synchronization and an ideal channel. In **Fig. 4**, the distribution is centered at a single point under perfect synchronization. However, in **Fig. 5**, $P_{RC}[k]$ of Method 1 spreads across all the FFT areas because of the effect of the SFO.

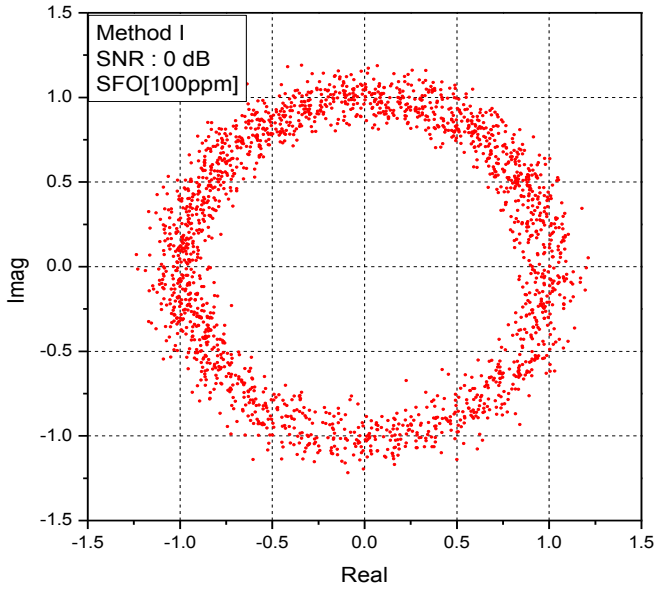

Fig. 4. $P_{RC}[k]/N$ phase shift due to SFO.

Then, the probability density function (PDF) of $\sum_{k=1}^{N_{RC}} H_{l_1}(P_{RC}[k])$ is analyzed to evaluate the frame detection performance. **Fig. 6** shows the PDF of Channel 3. l_1 is decided depending on $\sum_{k=1}^{N_{RC}} H_{l_1}(P_{RC}[k])$. $H_{l_1}(P_{RC}[k])$ is $E\left[H_{l_1}(P_{RC}[k])\right]=0$; because it is a wise-sense stationary process, $\left|\sum_{k=1}^{N_{RC}} H_{l_1}(P_{RC}[k])\right|$ becomes smaller as N_{RC} increases, resulting in frame detection performance degradation.

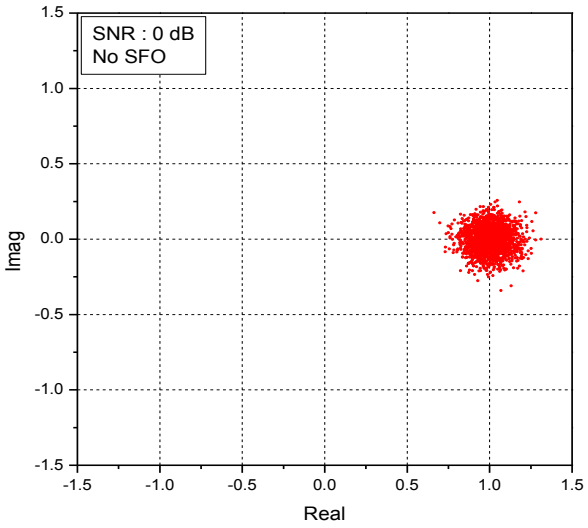

Fig. 5. $P_{RC}[k]/N$ phase shift in the absence of SFO.

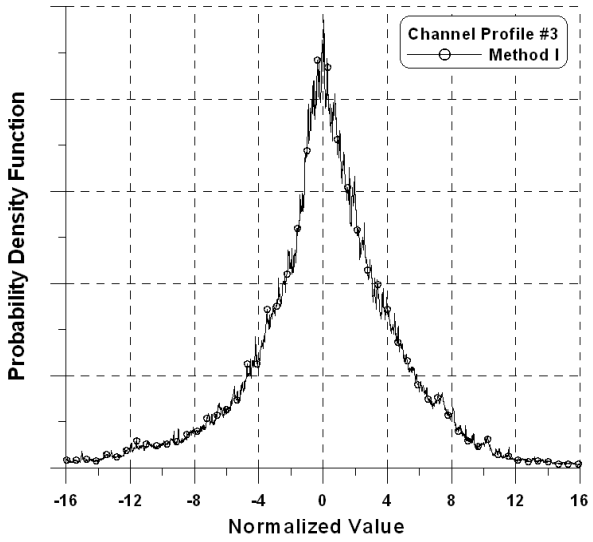

Fig. 6. Channel impulse response PDF for Method 1.

3.2 Method 2: Algorithm using Inter-carrier Differential Correlation Method

Method 2 does not perform initial SFO estimation and correction; thus, the synchronization speed increases. Because the initial detection and correction of the sampling frequency are omitted, the OFDM symbol after FFT may include the SFO, causing synchronization performance degradation in subsequent steps. Therefore, the IFO estimation and frame detection methods, which reduce the effects of SFO, are used to prevent degradation in the synchronization performance. After the initial synchronization, the STO, CFO, and SFO are repeatedly tracked and corrected [13].

To estimate the SFO, a minimum number of symbols must be observed, and the estimated SFO must be corrected. This process consumes synchronization time. For example, we

assume that the value of the SFO needed for receiver development is 10 ppm and the current estimated SFO is approximately 50 ppm. To correct for the required 10 ppm, Method 1 must observe approximately 35 symbols and must perform the correction to guarantee the performance [10]. Method 2 does not perform the initial SFO estimation and correction; hence, the synchronization speed increases.

Method 2 is an inter-carrier differential correlation method that obtains the correlation between the received reference cell and its subsequent reference cell [14]. Method 2 can be expressed as follows:

$$\hat{l}_2 \arg\max_{l_2} \left| \sum_{k=1}^{N_{RC}-1} R_{l_2}\left(P_{RC}[k]\right) \cdot R_{l_2}{}^{*}\left(P_{RC}[k+1]\right) \cdot e^{j2\pi\theta_{diff}(k)} \right| \tag{5}$$

where $e^{j2\pi\theta_{diff}(k)}$ is the phase difference between the consecutive reference cells, which is defined as follows:

$$e^{j2\pi\theta_{diff}(k)} = \angle X_{l_2}\left(P_{RC}[k]\right) \cdot X_{l_2}{}^{*}\left(P_{RC}[k+1]\right). \tag{6}$$

The distance between the reference cell and the next reference cell in Method 2 is small. Therefore, the phase change is also relatively small. Further numerical analysis of the received reference cell is presented as follows:

$$\begin{aligned} & R_{l_2}\left(P_{RC}[k]+m\right) \cdot R_{l_2}{}^{*}\left(P_{RC}[k+1]\right) \\ &= \left(\frac{N-\xi \cdot N_s \cdot l_2}{N}\right)^2 \cdot 2 \cdot e^{j2\pi\left(\xi \cdot N_s \cdot l_2\right)\left(P_{RC}[k]-P_{RC}[k+1]\right)/N} \cdot e^{j2\pi\left(l_2 \cdot N_s/N\right)\varepsilon} \\ & \quad \cdot X_{l_2}\left(P_{RC}[k]\right) \cdot X_{l_2}{}^{*}\left(P_{RC}[k+1]\right) \cdot H_{l_2}(P_{RC}[k]) \cdot H_{l_2}{}^{*}(P_{RC}[k+1]) \end{aligned} \tag{7}$$

In Equation (7), $X_{l_2}\left(P_{RC}[k]\right) \cdot X_{l_2}{}^{*}\left(P_{RC}[k+1]\right)$ is a known reference cell signal. Therefore, it can be eliminated by multiplying with $e^{j2\pi\theta_{diff}(k)}$. The result is shown below.

$$\begin{aligned} & R_{l_2}\left(P_{RC}[k]+m\right) \cdot R_{l_2}{}^{*}\left(P_{RC}[k+1]\right) \cdot e^{j2\pi\theta_{diff}(k)} \\ &= \left(\frac{N-\xi \cdot N_s \cdot l}{N}\right)^2 \cdot 2 \cdot e^{j2\pi\left(\xi \cdot N_s \cdot l_2\right)\left(P_{RC}[k]-P_{RC}[k+1]\right)/N} \cdot e^{j2\pi\left(l_2 \cdot N_s/N\right)\varepsilon} \\ & \quad \cdot H_{l_2}(P_{RC}[k]) \cdot H_{l_2}{}^{*}(P_{RC}[k+1]) \end{aligned} \tag{8}$$

The final frame detection result can be obtained by substituting Equation (8) into Equation (5) as shown below.

$$\begin{aligned} \hat{l}_{l_2} &= \arg\max_{l_2} \frac{N-\xi \cdot N_s \cdot l_2}{N} \cdot e^{j2\pi\left(l_2 \cdot N_s/N\right)\varepsilon} \left| \sum_{k=1}^{N_{RC}} e^{j2\pi\left(\xi \cdot N_s \cdot l_2\right)\left(P_{RC}[k]-P_{RC}[k+1]\right)/N} \cdot H_{l_2}(P_{RC}[k]) \cdot H_{l_2}(P_{RC}[k+1]) \right| \\ &= \arg\max_{l_2} \beta_{l_2} \cdot \left|\Gamma_{l_2}\right| \end{aligned} \tag{9}$$

where $\beta_{l_2} = \frac{N-\xi \cdot N_s \cdot l_2}{N} \cdot e^{j2\pi(l_2 \cdot N_s/N)\varepsilon}$ and $\Gamma_{l_2} = \sum_{k=1}^{N_{RC}} e^{j2\pi(\xi \cdot N_s \cdot l_2)(P_{RC}[k]-P_{RC}[k+1])/N} \cdot H_{l_2}(P_{RC}[k]) \cdot H_{l_2}(P_{RC}[k+1])$. The residual frequency offset value (ϵ) and the SFO in β_{l_2} are very small (in parts per million). Therefore, the approximations $\xi \lll 1$ and $\beta_{l_2} \approx 1$ hold. Applying these approximations to Equation (9) yields the following equation:

$$\hat{l}_2 = \arg\max_{l_2} \left| \Gamma_{l_2} \right|. \tag{10}$$

Equation (9) shows that $P_{RC}[k] - P_{RC}[k+1]$ is different from $P_{RC}[k]$ in the frame detection [Equation (3)] for Method 1. $P_{RC}[k]$ of Method 1 is influenced by the SFO that depends on the location of the reference cell in the total FFT domain. $P_{RC}[k] - P_{RC}[k+1]$ in Method 2 is influenced by the SFO that depends on the difference between the reference cell and the adjacent reference cell. Therefore, Method 2 is less affected by the SFO. **Fig. 7** shows the distribution of the phase shift of $P_{RC}[k] - P_{RC}[k+1]$ assuming an ideal channel. The distribution is centered at a particular area. The phase shift depends on the difference $P_{RC}[k] - P_{RC}[k+1]$; it is less influenced by the SFO compared with that in Method 1.

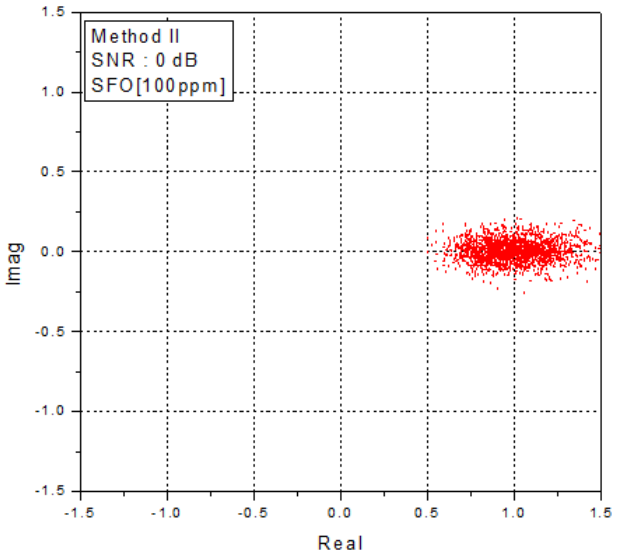

Fig. 7. $P_{RC}[k] - P_{RC}[k+1] / N$ phase shift due to SFO.

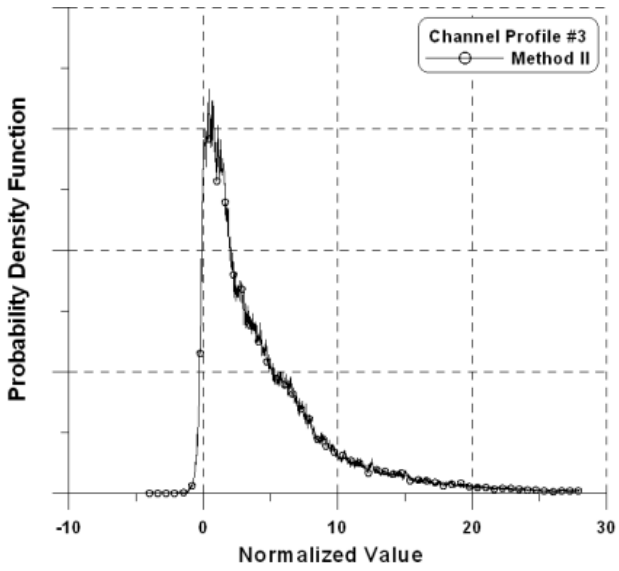

Fig. 8. Channel impulse response PDF for Method 2.

Another difference is presented by $H_{l_1}(P_{RC}[k])$ of Γ_{l_1} and $H_{l_2}(P_{RC}[k]) \cdot H_{l_2}{}^{*}(P_{RC}[k+1])$ of Γ_{l_2}. We observe the PDF of $H_{l_2}(P_{RC}[k]) \cdot H_{l_2}{}^{*}(P_{RC}[k+1])$ to analyze the performance, similar to that performed in Method 1. **Fig. 8** shows the PDF of $H_{l_2}(P_{RC}[k]) \cdot H_{l_2}{}^{*}(P_{RC}[k+1])$. Depending on the correlation of the nearby reference cells, the expected values do not exist in the negative domain. Unlike $H_{l_1}(P_{RC}[k])$ of Γ_{l_1}, $H_{l_2}(P_{RC}[k]) \cdot H_{l_2}{}^{*}(P_{RC}[k+1])$ of Γ_{l_2} has an average value of $E\left[H_{l_2}(P_{RC}[k]) \cdot H_{l_2}{}^{*}(P_{RC}[k+1])\right] = 4.5484$. We can see that it always has values greater than those in Method 1. Therefore, its performance is better than that of Method 1. The IFO estimation is $P_{RC}[k] = P_{RC}[k] + m$ from Equations (2) and (4). It can be estimated by finding m that maximizes the correlation value. In this case, the same performance evaluation result can be obtained by performing the same process as the frame detection.

4. Simulation Results

We have simulated how much time is required to estimate the initial SFO from the DRM signal and compared the frame detection performance based on the initial SFO of Methods 1 and 2 through simulations. We first measured the required number of symbols for the initial SFO estimation and compensation. A feedback structure [15] was applied for the sampling frequency estimation and compensation. Simulation was performed under the same condition shown in **Table 2**. We set the loop gain as one-fourth for stable tracking during feedback.

Fig. 9 shows the SFO estimation based on the number of OFDM symbols for 100, 50, and 10 ppm as initial SFOs under DRM mode B. The number of required symbols for estimation and compensation dramatically increases as the SFO increases. Table 3 shows the number of symbols to observe for the estimation and compensation with margins of error of 50, 10, and 5 ppm for 100, 50, and 10 ppm as SFOs, respectively.

Table 2. Experimental parameters for estimation and compensation of the initial SFO

Parameters	Condition/Value
Pulse Shaping Filter	Raised Cosine Filter
	Roll Off Factor : 0.3
	128 Over Sampling
Channel	AWGN Channel
	SNR : 0 dB
Loop Gain	1 / 4

Table 3 shows that the number of required symbols for estimation and compensation with a margin of error of 50 ppm is 28 with 100 ppm as the initial SFO; 79 symbols should be observed to estimate and compensate for a margin of error of 5 ppm. Under DRM mode B, Method 2 reduces the required time for initial synchronization with the amount of symbol time range (26.66 ms in this case) proportional to the number of observed symbols. The goal of the compensation offset (in parts per million) is generally determined by the required performance indicator from each receiver.

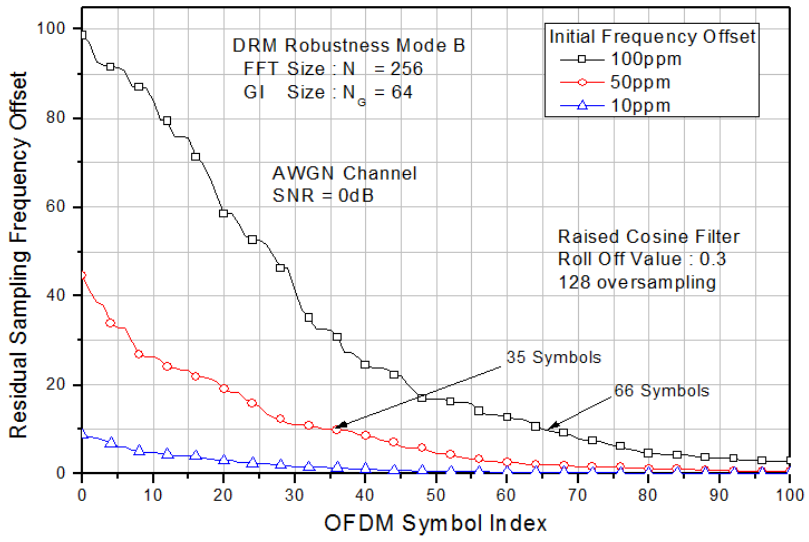

Fig. 9. Relationship between the number of observed symbols and SFO estimation and compensation.

Table 3. Number of required symbols for compensation offset according to SFO

Initial sampling freq. offset / Residual sampling freq. offset	10 ppm	50 ppm	100 ppm
50 ppm			27
10 ppm		35	66
5 ppm	12	48	79

The frame detection performance is evaluated when the SFO is present. The channel environment used for the simulation is shown in **Table 4**. Channel 1 is an additive white Gaussian noise (AWGN) channel. Channel 2 is a multipath Rician channel [1].

Table 4. Considered channel profile

	Channel 1	Channel 2	
Number of Paths	1	2	
Delay (ms)	0	0	1
Path Gain (dB)	1	1	0.5
Doppler Shift	0	0	0
Doppler Spread (Hz)	0	0	0.1

Fig. 10 and **11** show the probability of detection failure due to the SFO of Methods 1 and 2 in Channels 1 and 2, respectively.

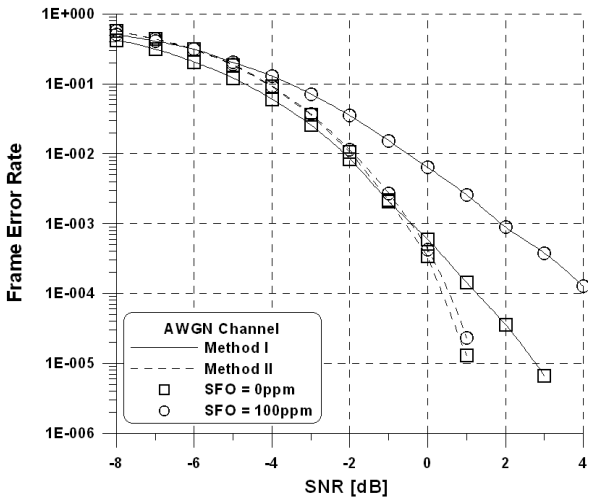

Fig. 10. Frame detection performance according to SFO (Channel 1).

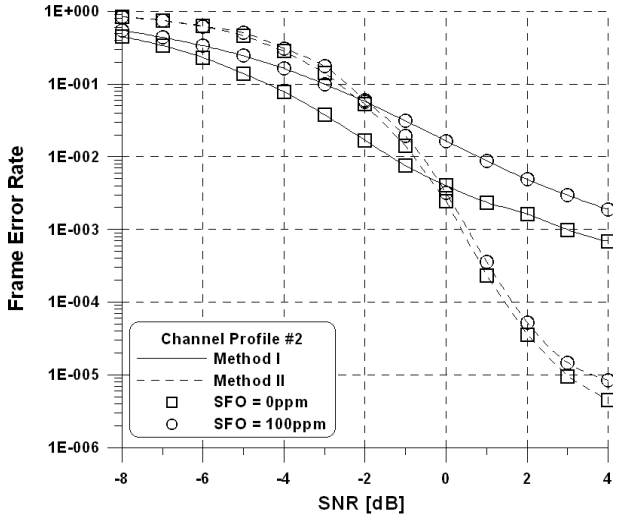

Fig. 11. Frame detection performance according to SFO (Channel 2).

In **Fig. 10**, if Method 1 is used under an AWGN environment, performance degradation occurs because of the effect of the SFO when the SFO increases from 0 to 100 ppm. Performance degradation is evident when the signal-to-noise power ratio (SNR) increases. However, in Method 2, the frame detection performance degradation is marginal even when the SFO increases. Therefore, Method 2 is less affected by the SFO. **Fig. 11** shows the frame detection performance in a multipath channel (Channel 2). Method 1 shows performance degradation as the SFO increases. Method 2 shows marginal degradation, similar to the result from the AWGN. Unlike the AWGN condition, no performance difference is observed in Method 1 when the SNR increases. An error floor occurs in Method 2 for high SNR. Compared with those in Method 1, the errors are larger in Method 2 for SNR values of −2 to 1.5 dB because the frequency response in the two consecutive reference cells and the noise difference are included in the differential correlation between consecutive reference cells within the same symbol in Method 2. However, Method 2 still shows good detection performance when the SNR is approximately 0 dB. Therefore, we found that Method 2 is suitable for the proposed synchronization architecture.

Additionally, we compared the performance from the addition and multiplication perspective to analyze the detection computational complexity of both Methods 1 and 2. In the case of complex multiplication, Method 2 requires a double complex multiplication compared with Method 1. Similarly, complex addition is required for both Methods 1 and 2. As a result, the computational complexity increases for Method 2, which requires double complex multiplication as compared with Method 1.

Table 5. Comparisons of computational complexity

	method 1	method 2
# of complex multiplications	$(2l+1)N_{RC}$	$2(2l+1)(N_{RC}-1)$
# of complex additions	$(2l+1)(N_{RC}-1)$	$(2l+1)(N_{RC}-2)$

5. Conclusion

In this paper, we have presented a comparative performance evaluation of the sampling frequency synchronization method that eliminates the initial SFO to reduce the overall synchronization time in DRM receivers. To satisfy the advanced synchronization performance requirements of DRM receivers, we introduced the conventional DRM synchronization method and another method that does not perform the initial sampling frequency synchronization process in the conventional synchronization method. We derived analytical expressions for frame detection and conducted simulations to demonstrate the effectiveness of the performance evaluation. We established a frame detection method that is not greatly influenced by the initial SFO in the DRM receivers. Method 1 required a long initial synchronization because of the initial SFO estimation and correction. From the frame-error-rate perspective, Method 2, with a negligible performance loss, did not perform initial SFO estimation and correction before FFT, reducing the synchronization duration. In addition, to detect a frame from the demodulated symbol with SFO, correlation algorithms were applied to the reference cells. The performance of the correlation algorithm robust to SFO was evaluated. The simulation results showed that when the differential correlation method was used between consecutive selected reference cells, it was robust to the effects of the initial SFO. The evaluated synchronization method in this paper was robust to the SFO effects and can be used as a key element technology in practical implementation of DRM receivers.

References

[1] ETSI ES 201 980, V 3.1.1, Digital Radio Mondiale (DRM); System Specification 2009. http://www.etsi.org/deliver/etsi_es/201900_201999/201980/03.01.01_50/es_201980v030101m.pdf

[2] T. Pollet, "The BER performance of OFDM systems using non-synchronized sampling," in *Proc. of* GLOBCOM'94, pp. 253-257. Dec. 1994. Article (CrossRef Link)

[3] F. Classen and H. Meyr, "Frequency synchronization algorithms for OFDM systems suitable for communication over frequency selective fading channels," in *Proc. of IEEE VTC*, pp. 1655-1659, June 1994. Article (CrossRef Link)

[4] M. Morelli and M. Moretti, "Integer frequency offset recovery in OFDM transmissions over selective channels," *IEEE Trans. Wireless Commun*., vol. 7, no.12, pp. 5220 -5226, Dec. 2008. Article (CrossRef Link)

[5] S. J. Kim, K. W. Park, S. H. Park, K. W. Kwon and J. H. Paik, "An effective frame detection and FFT window point tracking algorithm for digital radio mondiale receivers," in *Proc. ICCE 2009*, pp. 1-2. Jan. 2009. Article (CrossRef Link)

[6] V. Fischer and A. Kurpiers, "Frequency synchronization strategy for a PC-based DRM receiver," in *Proc. APCCS 2004*, pp. 989-992. Dec. 2004. http://citeseerx.ist.psu.edu/viewdoc/summary?doi=10.1.1.11.1643

[7] M. M. Freda, J. F. Weng, and T. Le-Ngoc, "Joint channel estimation and synchronization for OFDM systems," in *Proc. IEEE VTC*, vol. 3, pp. 1673-1677, Sep. 2004. Article (CrossRef Link)

[8] J. J. van de Beek, M. Sandell, and P. O. Borjesson, "ML estimation of time and frequency offset in OFDM systems," *IEEE Trans. Commun.*, vol. 45, no. 7, pp. 1800-1805, July 1997. Article (CrossRef Link)

[9] F. Hofmann, C. Hansen, and W. Schafer, "Digital Radio Mondiale(DRM) digital sound broadcasting in the AM bands," *IEEE Trans. Broad*., vol. 49, no. 3, pp. 319-328, Sept. 2003. Article (CrossRef Link)

[10] M. Speth, S. A. Fechtel, G. Fock, and H. Meyr, "Optimum receiver design for wireless broad-band systems using OFDM-Part I," *IEEE Trans. Commun.*, vol.47, no. 11, pp. 1668-1677, Nov. 1999. Article (CrossRef Link)
[11] M. Speth, S. A. Fechtel, G. Fock, and H. Meyr, "Optimum receiver design for OFDM-based broadband transmission—Part II: A case study," *IEEE Trans. Communi.*, vol. 49, no. 4, pp. 571–578, Apr. 2001. Article (CrossRef Link)
[12] H. Nogami and T. Nagashima, "A frequency and timing period acquisition technique for OFDM systems," in *Proc. IEEE PIMRC*, pp. 1010-1015. Sep. 1995. Article (CrossRef Link)
[13] H.S. Kim, S. J. Kim, Y. L. Lee and J. S Seo, "An effective frame synchronization technique in European digital radio for band I & II frequencys," in *Proc. IEEE BMSB*, pp. 1-4. June 2011. Article (CrossRef Link)
[14] HK. S. Woo, K. I. Lee, J. H. Paik, K. W. Park, W. Y. Yang and Y. S Cho, "A DSFBC-OFDM for a next generation broadcasting system with multiple antennas," *IEEE Trans. Broadcast*., vol. 53, no.2, pp. 539-546. June 2007. Article (CrossRef Link)
[15] T. Pollet and M. Peeters, "Synchronization with DMT modulation," *IEEE Communi. Mag.*, vol. 37, no. 4, pp. 80–86, Apr. 1999. Article (CrossRef Link)

Ki-Won Kwon received B.S. and M.S. degrees in computer engineering from Kwangwoon University, Korea, in 1997 and 1999, He also received the Ph.D. degree in the School of Electrical & Electronics Engineering from Chung-Ang University, Korea, in 2011. In 1999, he joined in KETI, Korea, where he is presently a managerial researcher at the Mobile Convergence Platform Research Center. His research interests are in the area of wireless/mobile communications and digital broadcasting systems.

Seong-Jun Kim received the B.S. degree in Electrical Engineering from Sungkyunkwan University, Korea in 2002, and the M.S. degree in Information and Communication from Sungkyunkwan University in 2004. He was a Research Engineer of Communication system Group, Samsung Thales by 2004. Since 2006, he has been with Mobile Convergence Platform Research Center in Korea Electronics Technology Institute (KETI), Korea. Since March 2011, He is also currently working toward to Ph.D. degree in Electrical Engineering at Sungkyunkwan University. His research interests are in the area of wireless/wired and mobile communication systems and broadcasting system.

Jun Hwang received the B.S and M.S. and Ph.D. degrees in Computer Science from Chung-Ang University, Korea, in 1985, 1987, and 1991 respectively. Since 1992, he has been a professor at the College of Information & Media of Seoul Women's University. His current interests are IPTV, convergence computing, and digital broadcasting.

Jong-Ho Paik received the B.S., M.S., and Ph.D. degrees in the school of Electrical and Electronic Engineering from Chung-Ang University, Seoul, Korea, in 1994, 1997, and 2007, respectively. He was a Director with Advanced Mobile Research Center at Korea Electronics Technology Institute (KETI) by 2011. He is currently an assistant professor in the department of multimedia, Seoul Women's University, since 2011. His research interests are in the areas of web-based communication system, wireless/wired communication system design, video communication system, software testing and advanced broadcasting/communication system.